Thermochimica Acta 510 (2010) 68–74

Contents lists available at ScienceDirect

Thermochimica Acta

journal homepage: www.elsevier.com/locate/tca

Solid state reactions of UO_2, ThO_2 and $(U,Th)O_2$ with ammonium nitrate

Meera Keskar*, T.V. Vittal Rao, S.K. Sali

Fuel Chemistry Division, Bhabha Atomic Research Centre, Trombay, Mumbai 400 085, India

ARTICLE INFO

Article history:
Received 19 March 2010
Received in revised form 21 June 2010
Accepted 23 June 2010
Available online 3 July 2010

Keywords:
Dissolution and separation
X-ray diffraction
Thermogravimetric analysis (TGA)
Differential thermal analysis

ABSTRACT

UO_2, ThO_2 and $(U_xTh_{1-x})O_2$ ($x = 0.1$ and 0.5) were reacted with NH_4NO_3 in different molar ratios up to 400 °C in air, to study the dissolution behavior. Solid state reaction of UO_2 with different moles of NH_4NO_3 showed various intermediate products, depending on the amount of NH_4NO_3. The end products at 400 °C were identified as U_3O_8 and UO_3, respectively when 1 and 1.5 mol of NH_4NO_3 were used. When UO_2 and NH_4NO_3 were reacted in 1:4 molar ratio, the intermediate products identified were $(NH_4)_2UO_2(NO_3)_4$ and $NH_4UO_2(NO_3)_3$ at 180 and 220 °C, respectively. XRD data of both the compounds were indexed on orthorhombic system. ThO_2 did not show any reaction with NH_4NO_3 up to 400 °C. The reaction of $(U,Th)O_2$ with 4 mol of NH_4NO_3 was studied to see the dissolution and separation of U from the mixed oxide. X-ray diffraction, thermal analysis and chemical analysis techniques were used for the characterization of the products.

1. Introduction

Thorium-based mixed oxide fuels $(U_xTh_{1-x})O_2$ are considered more promising advanced fuels in Indian nuclear power program, as these fuels have better thermo-physical and thermo-chemical properties compared to pure oxide fuels [1–5]. In the nuclear fuel cycle, fuel reprocessing is one of the important steps, to recover valuable actinide materials from the irradiated fuel. A well known aqueous process THOREX (Thorium–Uranium Extraction) is used for the separation of U from the bulk of Th [6]. This process is time consuming and produces a large quantity of highly radioactive liquid waste containing hazardous hard gamma emitting radionuclides [1]. Recently, a new pyrochemical method was developed for use on a pilot scale for reprocessing spent nuclear fuel and based on molten alkali metal carbonates [7].

Dissolution of the spent fuel is an important preliminary step for the separation of fuel elements from other fission products. Since mixed oxide UO_2–ThO_2 forms complete range of solid solution (0–100 mol%) [8], it is necessary to know the dissolution behavior of these mixed oxides. Dissolution of sintered ThO_2 in HNO_3 is possible only in the presence of HF [9], but presence of these ions is undesirable during reprocessing, as they corrode the dissolver vessels.

Keskar et al. have extensively studied the solid state reactions of different salts with actinide fuel oxides and their mixed oxides in various molar proportions, to identify the formation of various species at different temperatures, which are amenable for easy dissolution and separation of the actinide elements in dilute acid [10–15]. Identification of the products formed during the reactions [12–14] was helpful in knowing the minimum temperature and amount of the salts required for bringing the actinide elements into soluble form.

The oxidation of uranium oxide using alkali metal nitrates has been extensively investigated in view of the possible application of nitrate melt for the pyrochemical reprocessing [16]. Toussaint and Avogadro [17] studied the reaction of UO_2 with melts of eutectic mixture of alkali metal nitrate and reported the formation of mixed uranates of general formula $Na_{2-x}M_xU_2O_7$ (M = Li, K and Cs). Volkovich et al. [18,19] found that uranium dioxide is oxidized further and faster when oxygen is bubbled into a carbonate melt to which a small amount of nitrate ions has been added. This is because nitrate acts in a catalytic manner to continually form the more active peroxide and superoxide species, which are mainly responsible for the molten salt oxidation of UO_2 to alkali metal diuranates [18].

A new chemical method called ammonium nitrate-melt-technique (ANMT) is reported by Topal to synthesise oxide compounds [20]. This method is based on dissolving the metal oxides in ammonium nitrate melt (an oxidizing agent) and combusting the material at lower temperature to give the desired product. This technique was successfully applied in different areas; such as for synthesis of superconducting, magnetic and semiconducting oxides [21]. Oxley et al. [22] have stated that NH_4NO_3 is highly reactive and completely decomposes after melting at 169 °C and leaving no solid residue after the reaction. He has studied the effect of various inorganic additives (carbonates, sulphates, oxalates, nitrates and phosphates) on thermal decomposition of ammonium nitrate using differential scanning calorimetry (DSC)

* Corresponding author. Fax: +91 22 25505151.
E-mail address: meerakeskar@yahoo.com (M. Keskar).

0040-6031/$ – see front matter © 2010 Elsevier B.V. All rights reserved.
doi:10.1016/j.tca.2010.06.024

and evolved gas analysis (EGA) techniques and showed that some additives impart (increase or decrease) the thermal stability of ammonium nitrate. In the present study, solid state reactions of UO_2, ThO_2 and $(U,Th)O_2$ were carried out with different molar proportions of NH_4NO_3 at various temperatures with an aim to optimize the temperature and amount of salt required to bring the fuel elements in soluble form in dilute nitric acid.

2. Experimental

U_3O_8 (nuclear grade) was used as a starting material for the synthesis of various uranium oxides. $UO_{2.00}$ was prepared by reducing U_3O_8 in Ar + 8% H_2 atmosphere at 800 °C for 4–5 h. U_3O_7 was obtained by heating UO_2 at 250 °C for 4 h in air. ThO_2 was obtained by the thermal decomposition of thorium oxalate at 800 °C. $(U_xTh_{1-x})O_2$ with $x = 0.1$ and 0.5 were prepared by co-precipitating (U+Th) as hydroxides by adding ammonia solution to the respective nitrate solutions, mixed in the required proportions. The hydroxides were filtered, dried and heated in Ar + 8% H_2 at 800 °C for 5 h. Sintered UO_2, ThO_2 and $(U_xTh_{1-x})O_2$ pellets with $x = 0.5$ (sintered at 1600 °C in Ar + 8% H_2 for 4 h, having 94% theoretical density) were supplied by Radio Metallurgy Division, BARC. All the un-sintered and sintered oxides were mixed separately with NH_4NO_3 in 0.17, 0.33, 0.85, 1, 1.5, 1.7, 2, 3 and 4 molar proportions. The reaction mixtures were well ground and heated in alumina boats in a furnace for different durations in air. O/U of the intermediate compounds was determined by heating UO_{2+x} samples in a thermoanalyser in moist Ar + 8% H_2 atmosphere up to 800 °C for 3 h. The precision of O/U analysis is within ±0.005. In order to determine the role of NH_4NO_3, mixtures of UO_2 with 1.5 and 2 mol of NH_4NO_3 were heated in a thermoanalyzer in high purity argon atmosphere at a rate of 5 °C/min up to 400 °C. The products were dissolved in conc. H_3PO_4 and O/U was determined chemically using potentiometric analysis of U(IV) and U(total) [23].

X-ray powder diffraction (XRD) patterns of heated products were recorded on a STOE diffractometer using graphite monochromatised Cu Kα1 (λ = 1.5406 Å) radiation. Simultaneous thermogravimetric (TG) and differential thermal analysis (DTA) curves of various reaction mixtures were recorded from room temperature to 400 °C on a Mettler Thermoanalyser (model: TGA/SDTA 851^e/MT5/LF1600) by heating the sample in alumina cups at a heating rate of 5 °C/min in a flowing stream of dry air. Thermoanalyser was calibrated using thermal decomposition of $CaC_2O_4{\cdot}H_2O$ to CaO from 25 to 1000 °C in air.

To study the quantitative dissolution, all the heated products formed at various temperatures were treated with 2 M HNO_3 and heated on a hot plate at 100 °C. The chemical analysis of uranium in solutions was done by redox titrimetry using Davies and Gray method [23]. The products containing thorium were dissolved in hot conc. HNO_3, containing few drops of conc. HF. The thorium content was determined by EDTA titration using xylenol orange as an indicator [24].

Specific surface area and porosity of uranium trioxide obtained with heat treatment of UO_2 (un-sintered and sintered) with 4 mol of NH_4NO_3 were determined by the BET method using Sorpotomatic-1990 (CE Instruments). Tap density of UO_3 powder was determined by filling the powder in a measuring cylinder and tapping the cylinder so that the powder gets packed very well without voids. By knowing the weight of packed powder and the volume it occupies, the tap density was measured.

Particle size distribution analyses of uranium oxides were done by dynamic light scattering (DLS) technique [25]. The DLS instrument is equipped with 15 mW solid state laser (635 nm). For the determination of particle size, uranium trioxide powders were dispersed ultrasonically in distilled water. The supernatant solutions having suspended particles were used for particle size analysis using DLS technique.

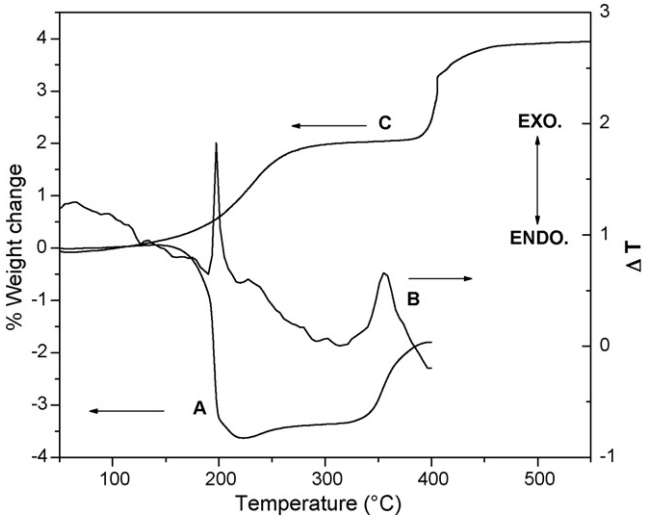

Fig. 1. (A) TG; (B) DTA curves for mixture of UO_2 and NH_4NO_3 in 1:0.17 molar ratio in air and (C) TG curve of UO_2 in air.

3. Results and discussion

3.1. Reactions of uranium oxide with ammonium nitrate

Thermal decomposition of ammonium nitrate in air was studied in detail by many workers using evolved gas analysis and differential scanning calorimetry [22,26,27]. The reported predominant decomposition reaction is shown below:

$$NH_4NO_3 \rightarrow N_2O + 2H_2O \quad (1)$$

The decomposition of ammonium nitrate in the temperatures range of 200–300 °C indicated the formation of various oxides of nitrogen in which N_2O is the first and main gas formed [28].

In the present work, thermogravimetric curve of NH_4NO_3 (AN) recorded in air showed 100% weight loss in a single step in the temperature range of 170–310 °C. DTA curve of the same showed two endothermic peaks at 70 and 120 °C corresponding to crystallographic phase transitions from room temperature orthorhombic phase to rhombohedral and cubic phases, respectively [26]. A sharp endothermic peak at 170 °C was due to melting and an endothermic DTA peak at 280 °C corresponded to decomposition of NH_4NO_3. This data is in agreement with the Notz and Hass [26].

Thermogram of a reaction mixture of UO_2 + 0.17 NH_4NO_3 in air is shown in Fig. 1. TG curve showed weight loss of 3.60% between the temperature range of 160–215 °C followed by a weight gain of 2.1% in the temperature range of 225–400 °C. XRD patterns of 200 and 400 °C heated products were similar to UO_2 and U_3O_8, respectively. O/U of the 200 °C heated product was found to be 2.2. In UO_2 + 0.17 NH_4NO_3 reaction, the decomposition of only NH_4NO_3 (0.17 mol) was expected to show the weight loss of 4.79% with endothermic DTA peak, but the observed weight loss was 3.60%. This could be due to the partial oxidation of UO_2 to $UO_{2.2}$ (expected total weight change for simultaneous decomposition of NH_4NO_3 and oxidation of UO_2 to $UO_{2.2}$ is 3.63%). The weight loss was associated with an exothermic DTA peak at 200 °C. The exothermic nature of DTA peak also substantiates the oxidation of UO_2 during decomposition of NH_4NO_3. The weight loss was followed by a weight gain in the temperature range of 225–400 °C associated with an exothermic DTA peak at 350 °C. This exothermic DTA peak was due to the oxidation of $UO_{2.2}$ to U_3O_8. In addition, DTA curve also showed endothermic

Table 1
Products identified and TG/DTA data observed during the reactions of UO_2, ThO_2 and $(U_xTh_{1-x})O_2$ with different molar proportions of NH_4NO_3 (AN).

Reactants	Temp. range (°C)	% Weight change from TG		Associated DTA peaks (°C)	Products identified by XRD
		Obs.	Cal.		
NH_4NO_3 (AN)	170–310	−100	−100	280 (endo)	–
UO_2 + 0.17 AN	160–215	−3.60	−3.63	200 (exo.)	UO_{2+x}
	225–400	+2.1	+2.48	350 (exo.)	U_3O_8
UO_2 + 0.33 AN	160–280	−7.06	−7.12	220 (exo.)	U_3O_7
	350–400	+1.64	+1.78	360 (exo.)	U_3O_8
UO_2 + 0.85 AN	160–280	−17.24	−17.75	220 (exo.)	$U_3O_7 + U_3O_8$
	300–400	+0.28	+0.76	360 (exo.)	U_3O_8
UO_2 + 1 AN	160–230	−12.87	−12.07	230 (exo.)	U_3O_8 + AN
	230–300	−6.88	−7.77	270 (endo.)	U_3O_8
UO_2 + 1.5 AN	170–255	−16.41	−16.48	250 (exo.)	UO_3 + AN
	255–310	−10.26	−11.79	280 (endo.)	α-UO_3
UO_2 + 1.7 AN	160–240	−15.28	−15.76	215 (exo.)	UO_3 + AN
	240–320	−14.27	−13.79	275 (endo.)	α-UO_3
UO_2 + 2 AN	180–250	−13.82	−14.88	210 (exo.)	UO_3 + AN
	250–330	−18.72	−18.60	280 (endo.)	α-UO_3
UO_2 + 3 AN	160–250	−21.44	−22.74	240 (exo.)	$UO_2(NO_3)_2$
	250–350	−20.72	−21.18	270 (endo.)	α-UO_3
UO_2 + 4 AN	160–230	−5.76	−6.10	200 (endo.)	$(NH_4)_2UO_2(NO_3)_4$
	230–260	−14.14	−13.56	225 (endo.)	$NH_4UO_2(NO_3)_3$
	260–400	−30.64	−31.86	285 (endo.)	α-UO_3
$UO_{2.66}$ + 4 AN	170–250	−6.9	−7.7	245 (endo.)	$(NH_4)_2UO_2(NO_3)_4$
	250–270	−13.01	−13.3	255 (endo.)	$NH_4UO_2(NO_3)_3$
	270–380	−30.6	−31.3	285 (endo.)	α-UO_3
ThO_2 + 4 AN	170–300	53.9	54.61	275 (endo.)	ThO_2
$(U_{0.1}Th_{0.9})O_2$ + 4 AN	180–300	54.11	54.46	270 (endo.)	$UO_3 + ThO_2$
Sint. $(U_{0.5}Th_{0.5})O_2$ + 4 AN	180–290	53.48	54.51	270 (endo.)	$(U_{0.5}Th_{0.5})O_2$

peaks at 125 and 170 °C, due to the phase transition and melting of NH_4NO_3, respectively. It is well known that when heated in air, UO_2 undergoes oxidation to form U_3O_7 as an intermediate oxide at 350 °C and on further heating up to 600 °C, gives U_3O_8 as the end product. To understand the role of oxygen from air in absence of ammonium nitrate, the oxidation of UO_2 was also carried out in thermoanalyser in a stream of dry air, heating UO_2 up to 600 °C and the resultant TG curve is shown in Fig. 1 for comparison. From the TG curves of UO_2 + 0.17 NH_4NO_3 and oxidation of UO_2 in air, it was confirmed that the second step oxidation (225–400 °C) in the former reaction is due to the oxidation of $UO_{2.2}$, formed during the decomposition of NH_4NO_3. It was confirmed that when heated with NH_4NO_3, the oxidation of UO_2 to U_3O_8 was complete at much lower temperature (400 °C) than in the air oxidation (600 °C). The products identified and TG/DTA data in different temperature ranges obtained during the reaction of UO_2 with 0.17 mol of NH_4NO_3 are given in Table 1.

TG curves of reaction mixtures of UO_2 with 0.33 and 0.85 mol of NH_4NO_3 also showed weight loss followed by a weight gain similar to the TG curve of UO_2 + 0.17 NH_4NO_3. The observed % weight losses and weight gains in each step during the above reactions are also included in Table 1. It can be seen from the table that during the reactions of UO_2 with 0.17, 0.33 and 0.85 mol of NH_4NO_3, % weight loss in the first step increases and % weight gain in the second step decreases with increase in number of moles of NH_4NO_3. The end product at 400 °C in all these reactions was identified as U_3O_8 indicating that the oxidation of UO_2 took place during the decomposition of NH_4NO_3. Higher the concentration of NH_4NO_3, more was the oxidation of UO_2 to UO_{2+x} in the first step, thereby reducing the % weight gain for the formation of U_3O_8 in second step. XRD patterns of the intermediate products isolated at 200 °C by reacting UO_2 with 0.33 and 0.85 mol of NH_4NO_3 matched with that of U_3O_7 and mixture of $U_3O_7 + U_3O_8$ having O/U values of 2.33 and 2.5, respectively. DTA curves of both the reaction mixtures were similar, showing two exothermic peaks at 220 and 360 °C due to the oxidation of UO_2 to UO_{2+x} and UO_{2+x} to U_3O_8, respectively. The three additional endothermic DTA peaks observed at 50, 125 and 155 °C, corresponded to the phase changes and melting of ammonium nitrate. This indicated that the reaction between UO_2 and ammonium nitrate starts after melting of ammonium nitrate.

Thus the reactions of UO_2 with 0.17, 0.33 and 0.85 mol of ammonium nitrate up to 400 °C showed the oxidation of UO_2 in two steps as revealed by thermogravimetric, O/U and XRD analysis. Oxidation of UO_2 in presence of ammonium nitrate in the temperature range of 160–240 °C was clearly indicated by an exothermic DTA peak in contrast to endothermic DTA peak observed during the decomposition of ammonium nitrate alone.

When the mixtures of UO_2 and NH_4NO_3 in the molar ratios of 1, 1.5, 1.7 and 2 were heated, the TG curves of all the mixtures showed weight losses in two steps, the former step being associated with exothermic and latter with endothermic DTA peak. In these reactions, no weight gain was observed up to 400 °C. XRD patterns of the products formed by reacting UO_2 with 1 mol of NH_4NO_3 at 250 and 400 °C were identified as a mixture of $U_3O_8 + NH_4NO_3$ and U_3O_8, respectively. However, when UO_2 was reacted with 1.5, 1.7 and 2 mol of NH_4NO_3 led to the formation of $UO_3 + NH_4NO_3$ and α-UO_3 at 250 and 400 °C, respectively. Formation of α-UO_3 was confirmed by XRD [29]. Apparently for the formation of UO_3 from UO_2 requires decomposition of 1 mol of NH_4NO_3, the decomposition of excess 0.5, 0.7 and 1.0 mol of ammonium nitrate showed weight losses in the second step. The strong exothermic DTA peak was due to the oxidation of UO_2 and an endothermic peak was due to the decomposition of excess NH_4NO_3. The decomposition of excess NH_4NO_3 started at higher temperature which may be because of the presence of UO_3. Similar shift in the decomposition temperature of NH_4NO_3 in presence of the additives like sulphate, carbonate, phosphate salts of sodium and potassium has been reported by Oxley

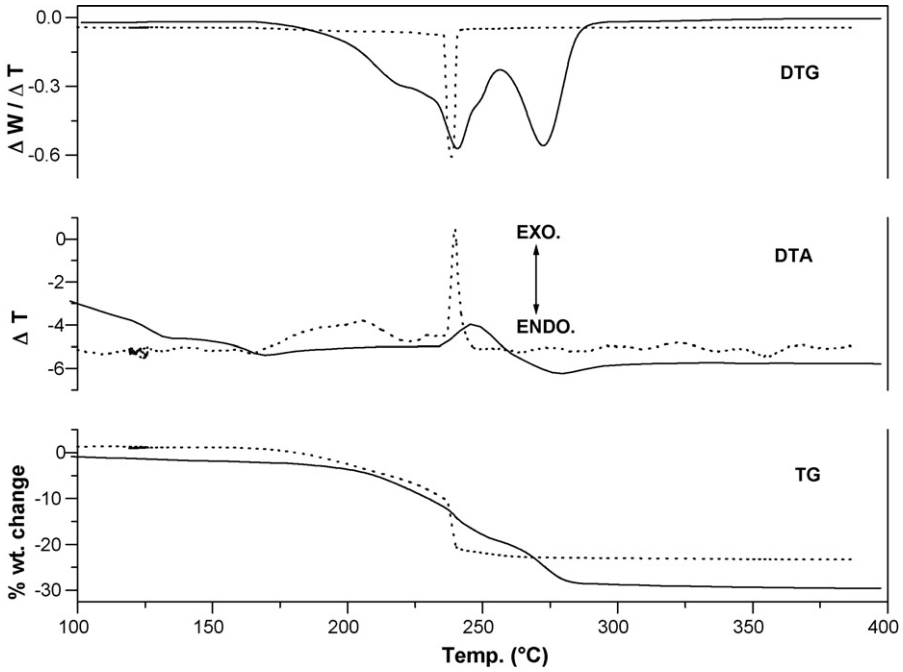

Fig. 2. TG, DTA and DTG curves for mixture of UO_2 and NH_4NO_3 in 1:1.5 molar ratio in air (solid lines) and in argon atmosphere (dotted line).

et al. [22]. All the weight changes and corresponding DTA temperatures are summarized in Table 1.

To check the role of NH_4NO_3 during the oxidation of UO_2, the oxide was mixed with 1.5 mol of NH_4NO_3 and was heated in high purity argon atmosphere. Fig. 2 shows the thermograms of UO_2 + 1.5 mol of NH_4NO_3 in air and argon atmosphere up to 400 °C at the heating rate of 5 °C/min. TG showed the weight loss in two steps in air and one step in argon and these steps were clearly resolved in DTG plots. Total % weight loss in argon atmosphere (23.93%) was less than that in air (26.67%). The decomposition of NH_4NO_3 was fast in Ar atmosphere and completed at lower temperature (240 °C) as compared to air (310 °C). This shift in temperature may be because of shift in equilibrium due to interference of N_2 from air with N_2 produced from decomposition of NH_4NO_3. The product identified at 300 °C indicated formation of $UO_{2.85}$ as determined by chemical analysis [23]. The DTA showed one and two exothermic peaks in air and argon atmosphere, respectively. The oxidation of UO_2 to $UO_{2.85}$ in argon atmosphere clearly showed that NH_4NO_3 plays a major role in oxidation.

In a separate experiment, when UO_2 was reacted with 2 mol of NH_4NO_3 in Ar atmosphere, the product obtained at 250 °C was UO_3, which was confirmed by chemical analysis and XRD. This shows that for the complete oxidation of UO_2 to UO_3 in inert atmosphere minimum 2 mol of NH_4NO_3 are required whereas in air it requires 1.5 mol of NH_4NO_3. This observation is in agreement with the results reported by Campbell et al. [30] and White et al. [31], where they mentioned that the rate of oxidation of UO_2 is enhanced in NO_2–O_2 gas mixture and can cause the oxidation to proceed beyond U_3O_8 to UO_3. Gas chromatographic analysis of the products formed from the reaction involving UO_2 and nitrate showed that the evolution of NO_2 and NO gases in air and inert atmospheres, respectively [19].

TG and DTA curves of UO_2 + 3 NH_4NO_3 are shown in Fig. 3. TG curve showed 21.44 and 20.72% weight losses in the temperature ranges 160–250 °C and 250–350 °C accompanied with an exothermic DTA peak at 240 °C and an endothermic peak at 270 °C, respectively. The exothermic peak was due to the oxidation of UO_2 whereas the endothermic peak was due to the complete decomposition of an intermediate product. As mentioned earlier, additional endothermic DTA peaks of NH_4NO_3 were also observed. XRD of the products isolated at 240 and 400 °C was identified as $UO_2(NO_3)_2$ and α-UO_3, respectively. The weight losses (obs. = 21.44%; cal. = 22.74%) were also in good agreement and confirmed the formation of $UO_2(NO_3)_2$ at 240 °C. Decomposition of uranyl nitrate to UO_3 was observed between 250 and 350 °C showing 20.72% weight loss which was in agreement with calculated weight loss of 21.18%. Notz and Hass [26] have also mentioned the formation of UO_3 by uranyl nitrate decomposition at around 270 °C. The observed and calculated weight losses along with the temperature ranges of decomposition are given in Table 1.

TG, DTA and DTG curves of UO_2 mixed with NH_4NO_3 in 1:4 molar ratio are shown in Fig. 4. TG curve showed weight losses in the three temperature ranges i.e. 160–230, 230–260 and 260–400 °C, each accompanied with an endothermic DTA peak at 200, 225 and 285 °C, respectively. The three step weight losses were also confirmed by associated DTG (dw/dt) and DTA peaks. The DTA showed additional

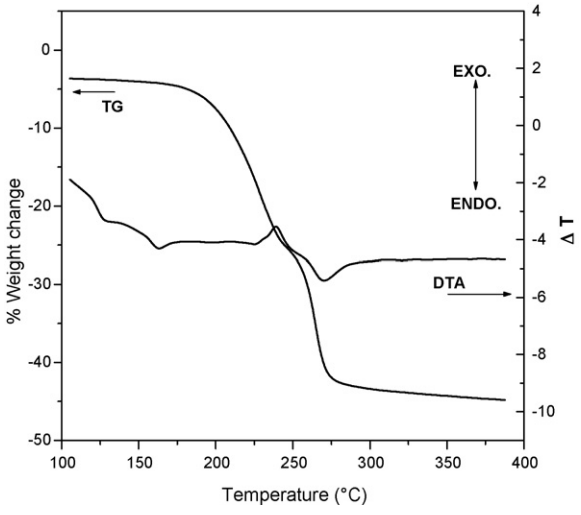

Fig. 3. TG and DTA curves for mixture of UO_2 and NH_4NO_3 in 1:3 molar ratio in air.

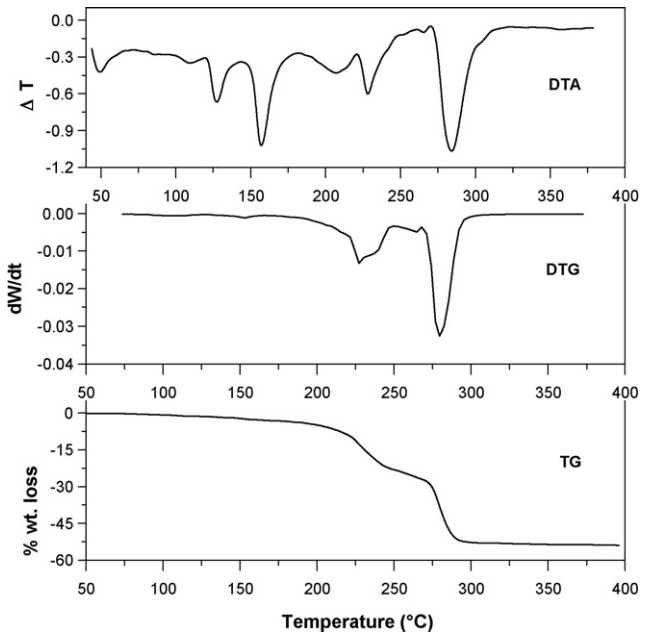

Fig. 4. TG, DTA and DTG curves for mixture of UO_2 and NH_4NO_3 in 1:4 molar ratio in air.

endothermic peaks at 50, 130 and 160 °C, due to NH_4NO_3. To isolate the intermediate products, the reaction mixture of UO_2 + 4 NH_4NO_3 was heated in the furnace in air at different temperatures. The product obtained at 180 °C was identified as $(NH_4)_2UO_2(NO_3)_4$ and its XRD data is comparable to those reported by Notz and Hass [26]. $(NH_4)_2UO_2(NO_3)_4$, when heated in furnace at 220 °C for 4 h, led to the formation of $NH_4UO_2(NO_3)_3$, which on further heating decomposes to α-UO_3 at 400 °C. The synthesis and decomposition of $(NH_4)_2UO_2(NO_3)_4$ is shown below:

$$UO_2 + 4NH_4NO_3 + 2O_2 \rightarrow (NH_4)_2UO_2(NO_3)_4 + N_2 + 4H_2O \quad (2)$$

$$(NH_4)_2UO_2(NO_3)_4 \rightarrow NH_4UO_2(NO_3)_3 + N_2O + 2H_2O \quad (3)$$

$$NH_4UO_2(NO_3)_3 \rightarrow UO_3 + N_2O_5 + N_2O + 2H_2O \quad (4)$$

Decomposition study of $(NH_4)_2UO_2(NO_3)_4{\cdot}2H_2O$ to UO_3, via ammonium uranyl tetra- and tri-nitrate as intermediate phases was reported by Kim et al. [32]. Thus, the present method can be used as an easy and simple alternative method, over the conventional ADU (ammonium diuranate) route for the preparation of UO_3. In the PDF data files the XRD data of $(NH_4)_2UO_2(NO_3)_4$ and $NH_4UO_2(NO_3)_3$ are not indexed [33,34] and therefore XRD data of both the compounds were indexed in the present study using a computer program [35]. The data of ammonium uranyl tetra- and tri-nitrate compounds were indexed on orthorhombic systems with refined lattice parameters of a = 9.354(5) Å, b = 13.177(9) Å, c = 10.372(5) Å and a = 12.540(8) Å, b = 7.076(3) Å, c = 17.532(9) Å, respectively. The measured densities of $(NH_4)_2UO_2(NO_3)_4$ and $NH_4UO_2(NO_3)_3$ i.e. $\rho_{obs.}$ = 2.87 and 3.93 g/cm^3 were determined by liquid displacement method using carbon tetrachloride as a solvent and are in good agreement with the theoretical densities, $\rho_{cal.}$ = 2.88 and 4.00 g/cm^3, respectively for four number of molecules per unit cell (Z). Indexed XRD data of $(NH_4)_2UO_2(NO_3)_4$ and $NH_4UO_2(NO_3)_3$ are given in Tables 2 and 3, respectively.

Thus it can be stated that solid state reactions of UO_2 with NH_4NO_3 lead to the formation of different intermediate products depending on the amount of NH_4NO_3 used.

Reaction of sintered UO_2 was also carried out with NH_4NO_3 in 1:4 molar ratio. The products formed at 180, 220 and 400 °C were similar to those obtained during the reaction of UO_2 with 4 NH_4NO_3. Thus, sintered UO_2 reacts with NH_4NO_3 forming α-UO_3 as the product, which can be easily dissolved in dil. HNO_3.

Table 2
X-ray diffraction data of $(NH_4)_2UO_2(NO_3)_4$. a = 9.354(5) Å, b = 13.177(9) Å, c = 10.372(5) Å, $\rho_{obs.}$ = 2.87 g/cm^3, Z = 4.

h	k	l	$d_{(obs.)}$ (Å)	$d_{(cal.)}$ (Å)	I/I_0
0	2	0	6.576	6.588	84
1	1	1	6.141	6.145	100
2	0	0	4.674	4.677	70
0	2	2	4.072	4.075	50
2	2	0	3.789	3.810	50
0	4	0	3.93	3.294	08
0	4	1	3.142	3.140	12
3	0	1	2.983	2.986	15
3	2	0	2.813	2.818	18
1	3	3	2.608	2.609	<5
2	2	3	2.562	2.561	10
4	0	0	2.338	2.338	22
0	6	0	2.199	2.196	08
1	3	4	2.177	2.174	11
3	3	3	2.047	2.048	07
2	1	5	1.877	1.877	15
1	3	5	1.837	1.839	10
3	6	1	1.767	1.769	<5
0	0	6	1.729	1.729	05
5	4	1	1.607	1.607	07

To identify the intermediate products and check the oxidation of hyper-stoichiometric uranium oxides, 4 mol of NH_4NO_3 were reacted with $UO_{2.12}$, $UO_{2.33}$ and $UO_{2.66}$ up to 400 °C in air. The weight loss calculations from TG curves confirm the formation of UO_3, via the formation of tetra and tri ammonium uranyl nitrate as an intermediate product. Each weight loss step was accompanied with an endothermic DTA peak similar to that observed in DTA curve of $UO_{2.00}$ + 4 NH_4NO_3. The observed weight losses along with the respective temperature ranges obtained during the heating of $UO_{2.66}$ with 4 mol of NH_4NO_3 are given in Table 1. It was confirmed that uranium oxide with O/U ranging from 2.0 to 2.66, can be easily oxidize to UO_3 by reacting with NH_4NO_3 in 1.5 or more molar proportion.

3.2. Reaction of ammonium nitrate with thorium oxide and uranium thorium mixed oxide

The reaction mixtures of 4:1 proportions of NH_4NO_3 with freshly prepared ThO_2 (obtained from thermal decomposition of

Table 3
X-ray diffraction data of $NH_4UO_2(NO_3)_3$. a = 12.540(8) Å, b = 7.076(3) Å, c = 17.532(9) Å, $\rho_{obs.}$ = 3.93 g/cm^3, Z = 4.

h	k	l	$d_{(obs.)}$ (Å)	$d_{(cal.)}$ (Å)	I/I_0
1	1	0	6.167	6.163	100
2	1	0	4.687	4.693	53
3	0	1	4.071	4.066	48
0	1	4	3.727	3.726	36
0	1	5	3.147	3.142	28
2	2	0	3.077	3.081	20
0	0	6	2.919	2.922	32
0	1	6	2.704	2.701	30
4	1	3	2.572	2.573	26
5	1	1	2.343	2.343	26
4	2	2	2.267	2.267	12
0	3	3	2.188	2.187	23
1	3	4	2.050	2.049	22
0	1	9	1.981	1.878	8
5	1	6	1.878	1.838	8
0	4	0	1.838	1.769	10
4	3	4	1.731	1.732	7
3	4	0	1.628	1.629	5
5	1	8	1.608	1.607	6
6	0	7	1.604	1.605	11

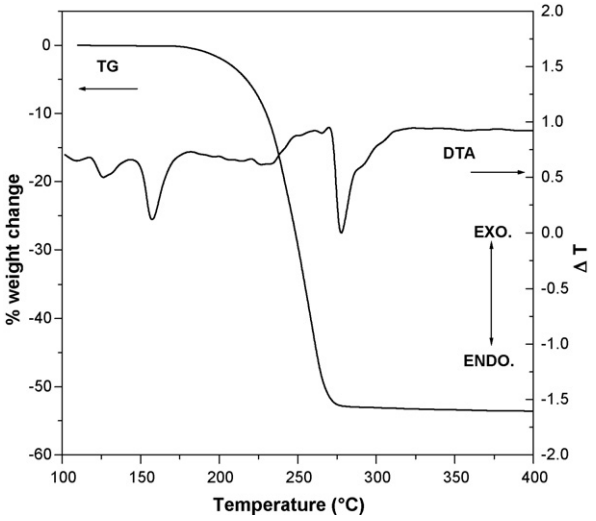

Fig. 5. TG and DTA curves for mixture of $(U_{0.1}Th_{0.9})O_2$ and NH_4NO_3 in 1:4 molar ratio in air.

$Th(C_2O_4)\cdot 6H_2O$ at 600 °C in air) and also sintered ThO_2 were heated in thermoanalyser as well as in the furnace up to 400 °C to check the reaction steps and the formation of intermediate products. TG curve of ThO_2 mixed with NH_4NO_3 in 1:4 molar ratio showed a single step weight loss of 53.9% between 170 and 300 °C corresponding to the loss of ammonium nitrate (calculated weight loss 54.61%). DTA curve showed endothermic peak at 275 °C due to the decomposition of NH_4NO_3 and additional three endothermic peaks similar to those observed in the DTA curve of NH_4NO_3. The products obtained by heating ThO_2 + 4 NH_4NO_3 at 200 °C and 400 °C in furnace, as well as the end product of thermal analysis were identified as ThO_2 indicating that there was no reaction between NH_4NO_3 and ThO_2. Similar results were also obtained with sintered ThO_2.

To check the reactivity of UO_2 and ThO_2 in mixed oxide, un-sintered $(U_xTh_{1-x})O_2$ with $x = 0.1$ and 0.5 was mixed with 4 mol of NH_4NO_3 and were heated in thermoanalyser up to 400 °C. TG curves of both reaction mixtures showed weight loss in a single step from 180 to 300 °C, accompanied by an endothermic DTA peak at 270 °C. The DTA curve showed additional endothermic peaks of NH_4NO_3. The products obtained at 400 °C were orange in color, indicated the oxidation of uranium. The products were analyzed by XRD and found to be a mixture of α-UO_3 and ThO_2. TG and DTA curves of $(U_{0.1}Th_{0.9})O_2$ + 4 NH_4NO_3 are shown in Fig. 5, where observed weight loss (54.11%) matched with the calculated weight loss (54.46%) corresponding to the formation of a mixture of α-UO_3 and ThO_2. Thus, it was confirmed that when mixed oxides $(U_xTh_{1-x})O_2$ are reacted with 4 mol of NH_4NO_3 at 400 °C, UO_2 gets oxidized to UO_3 whereas ThO_2 remains unreacted.

Further, with an aim to separate uranium from thorium in the spent fuel, reaction of 1600 °C sintered $(U_{0.5}Th_{0.5})O_2$ was carried out with 4 mol of NH_4NO_3. When the reaction mixture was heated in thermoanalyser, TG curve showed a single step weight loss between 180 and 290 °C (53.48%) and an endothermic DTA peak at 265 °C. Additional DTA peaks at 50, 120 and 170 °C were observed due to the phase transition and melting of NH_4NO_3. The XRD of the end product was identified as $(U_{0.5}Th_{0.5})O_2$ solid solution. Thus, a single step observed weight loss was due to the loss of NH_4NO_3 (calculated weight loss = 54.51%). From thermogravimetric and XRD analyses, it was concluded that uranium from un-sintered mixed oxide gets easily oxidized by reacting with 4 mol of NH_4NO_3, whereas in sintered oxide, uranium is not oxidized.

3.3. Dissolution and separation of uranium in mixed oxide

To check the solubility of the oxides, all 400 °C heated products formed during the reactions of un-sintered UO_2, ThO_2 and $(U_{0.1}Th_{0.9})O_2$ as well as sintered UO_2 and $(U_{0.5}Th_{0.5})O_2$ with 4 mol of NH_4NO_3 were treated with hot 2 M HNO_3. Uranium in the solutions was determined by potentiometric method and thorium by EDTA titration. As uranium interferes during analysis of thorium by EDTA titration method [24], thorium in the solution was separated by precipitating it as thorium oxalate whereas uranium(VI) does not precipitate with oxalic acid. The results of analyses of uranium and thorium are given in Table 4.

As seen from the Table 4, all the uranium from UO_2 and un-sintered $(U_{0.1}Th_{0.9})O_2$ could be brought in the soluble form quantitatively. Un-sintered, sintered ThO_2 as well as thorium from $(U_{0.1}Th_{0.9})O_2$ mixed oxide showed negligible solubility.

It can be mentioned here that sintered UO_2 could be easily brought in soluble form by reacting with 4 mol of NH_4NO_3 at 400 °C.

Table 4 also shows that the products obtained by reacting sintered $(U_{0.5}Th_{0.5})O_2$ with 4 NH_4NO_3 showed very less solubility for uranium compared to that in un-sintered mixed oxides.

3.4. Specific surface area/porosity and particle size determination

UO_3 is formed as an intermediate compound during the thermal decomposition of ammonium diuranate $[(NH_4)_2U_2O_7$, ADU], ammonium uranyl carbonate $[(NH_4)_2UO_2(CO_3)_2\cdot 2H_2O$, AUC], uranium peroxide $[H_2UO_5\cdot 5H_2O$, UP], uranyl nitrate hexahydrate $[UO_2(NO_3)_2\cdot 6H_2O$, UNH], etc., in the temperature range of 350–450 °C. Uranium dioxide powder, obtained by reduction of UO_3 in Ar + H_2 atmosphere, is used either for fabrication of nuclear fuel or for uranium metal production. The properties of the final product depend upon the nature of precursor and its thermal treatment [36]. The specific surface area, porosity, particle size and tap density of UO_3 derived from various preparatory conditions are given in Table 5. It can be seen from the table that the specific surface area, porosity, particle size and tap density of UO_3 obtained from the reaction of un-sintered UO_2 + 4 NH_4NO_3 at 400 °C were 5–6 m^2/g, 0.007 cm^3/g, 1.0 μm and 1.7 g/cm^3, respectively. The smaller particle size (1 μm) associated with the low value of porosity (0.007cm^3/g) and relatively moderate tap density (1.7 g/cm^3) indicated the formation of free-flowing compact powder which is suitable for the fabrication of high density UO_2 pellet. The values of specific surface area, porosity, particle size

Table 4
Chemical analysis of uranium and thorium from the products obtained by reacting UO_2, ThO_2 and $(U,Th)O_2$ with 4 mol of NH_4NO_3 at 400 °C.

U/Th oxides	Metal content in oxide (mg)		Metal content analysed from dissolved product (mg)		% of metal determined	
	U	Th	U	Th	U	Th
UO_2	434.30	–	431.06	–	99.25	–
Sintered UO_2	201.65	–	199.61	–	98.99	–
ThO_2	–	198.90	–	4.87	–	2.05
Sintered ThO_2	–	175.70	–	2.81	–	1.60
$(U_{0.1}Th0_{.9})O_2$	35.70	197.20	34.68	4.81	97.14	1.44
Sintered $(U_{0.5}Th_{0.5})O_2$	99.74	101.06	16.83	3.20	13.87	1.07

Table 5
Physical characteristics of UO_3 derived from various preparative conditions.

UO_3 obtained from	Specific surface area (m^2/g)	Porosity (cm^3/g)	Avg. particle size (μm)	Tap density (g/cm^3)	Ref.
Uranly nitrate	0.2–3	–	2.5–3.6	–	[31]
Ammonium diuranate	10–11	–	15	2.2	[33]
Sol–gel	28–31	0.028	1.1–1.5	0.93	[32]
UO_2 + 4 AN	5–6	0.007	1–2	1.7	Present work
Sintered $UO_{2.00}$ + 4 AN	1–2	0.002	7–9	1.4	Present work

and tap density of UO_3 derived from the reaction of UO_2 + 4 AN at 400 °C are comparable with those of UO_3 obtained from sol–gel and ADU methods, conventionally used for fabrication of UO_2 pellets [37,38]. However, the reaction of sintered UO_2 + 4 AN gave bigger sized UO_3 particles (9 μm) having relatively less surface area (1.5 m^2/g) and tap density. Thus, these data show that UO_3 obtained from reactions of un-sintered UO_2 with ammonium nitrate gives better powder characteristics as compared to that of sintered UO_2.

4. Conclusions

Solid state reactions of uranium oxides with NH_4NO_3 indicated that the oxidation takes place after melting of NH_4NO_3, leading to the formation of UO_{2+x}, where the value of x depends on the amount of NH_4NO_3. A simple and fast method was developed for synthesis of UO_3, by heating uranium oxide (O/U = 2–2.66) with 1.5 or more moles of NH_4NO_3 in air, up to 400 °C. Sintered UO_2 also reacted easily with 4 mol of NH_4NO_3 at 400 °C forming UO_3 which was readily soluble in dil. HNO_3. ThO_2 did not react with NH_4NO_3 up to 400 °C and thus when un-sintered mixed oxide $(U_x,Th_{1-x})O_2$ was reacted with 4 mol of NH_4NO_3 up to 400 °C, only uranium was oxidized and was soluble whereas ThO_2 remained insoluble in the residual form.

Acknowledgments

The authors are thankful to Dr. V. Venugopal, Director, Radiochemistry and Isotope Group for his keen interest in this work. Thanks are due to Dr. S.K. Aggarwal, Head, Fuel Chemistry Division, for critical reading of manuscript. The authors also thank Dr. S. Kannan, Head, X-ray and Structural Studies Section and Dr. S.K. Mukerjee, Head, Process Chemistry Section, for their constant encouragement and useful suggestions throughout this work. Authors are also thankful to Shri Rajesh Pai for providing data on particle size measurements.

References

[1] R.K. Sinha, A. Kakodkar, Nucl. Eng. Des. 236 (2006) 683.
[2] H. Gruppelaar, J.P. Schapira (Eds.), Project Report EUR 19412, Thorium as a waste management option, Nuclear Science and Technology Series, 2000.
[3] B. Fourest, T. Vincent, G. Lagarde, S. Hubert, P. Boudoin, J. Nucl. Mater. 282 (2000) 180.
[4] S. Hubert, K. Barthelet, B. Fourest, G. Lagarde, N. Dacheux, N. Baglan, J. Nucl. Mater. 206 (2001) 97.
[5] V. Neck, J.I. Kim, Radiochim. Acta 89 (2001) 206.
[6] W.W. Schultz, L.L. Buger, J.D. Navratil, K.P. Bender (Eds.), Applications of Tributyl Phosphate in Nuclear Fuel Processing, Science and Technology of Tributyl Phosphate, vol. (iii), CRC Press Inc., Florida, 1990.
[7] T.R. Griffiths, V.A. Volkovich, Nucl. Technol. 163 (2008) 382.
[8] E. Zimmer, E. Merz, J. Nucl. Mater. 124 (1984) 64.
[9] K. Vijayan, Annual Conference of Indian Nuclear Society (INSAC), Mumbai, 2000, p. 50.
[10] M. Keskar, U.M. Kasar, K.D. Singh Mudher, V. Venugopal, J. Nucl. Mater. 282 (2000) 146.
[11] M. Keskar, U.M. Kasar, K.D. Singh Mudher, V. Venugopal, J. Nucl. Mater. 334 (2004) 207.
[12] K.D. Singh Mudher, M. Keskar, N.C. Jayadevan, J. Nucl. Mater. 218 (1995) 166.
[13] K.D. Singh Mudher, M. Keskar, V. Venugopal, J. Nucl. Mater. 265 (1999) 146.
[14] S. Chaudhury, M. Keskar, A. Patil, K.D. Singh Mudher, V. Venugopal, Radiochim. Acta 94 (2006) 357.
[15] M. Keskar, K.D. Mudher Singh, V. Venugopal, J. Nucl. Mater. 336 (2005) 40.
[16] T. Fujino, K. Ouchi, T. Yamashita, H. Natsume, J. Nucl. Mater. 116 (1983) 157.
[17] C.J. Toussaint, A. Avogadro, J. Inorg. Nucl. Chem. 36 (1972) 781.
[18] V. Volkovich, T.R. Griffiths, D.J. Fray, M. Fields, J. Nucl. Mater. 256 (1998) 131.
[19] V. Volkovich, T.R. Griffiths, D.J. Fray, M. Fields, P.D. Wilson, J. Chem. Soc. Faraday Trans. 92 (1996) 5059.
[20] U. Topel, J. Phys.: Conf. Ser. 153 (2009) 012031.
[21] U. Topal, H. Ozkan, H.I. Bakan, O. Cankur, K. Topal, J. Non-Cryst. Solids 354 (2008) 1678.
[22] J.C. Oxley, J.L. Smith, E. Rogers, M. Yu, Thermochim. Acta 384 (2002) 23.
[23] W. Davies, W. Gray, Talanta 11 (1964) 1203.
[24] A. Ramanujam, P.S. Dhami, V. Gopalkrishnan, A. Mukherjee, R.K. Dhumwad, Report B.A.R.C.-1486, Bhabha Atomic Research Centre, 1989.
[25] B. Berne, R. Pecora, DLS with Applications to Chemistry, Biology and Physics, Wiley Interscience, New York, 1976.
[26] K.J. Notz, P.A. Haas, Thermochim. Acta 155 (1989) 283.
[27] J.C. Oxley, S.M. Kaushik, N. Gilson, Thermochim. Acta 153 (1989) 269.
[28] J.H. Oh, D.S. Hwang, K. Lee II, Y.D. Choi, S.T. Hwang, J.H. Park, S.J. Park, J. Ind. Eng. Chem. 12 (2006) 682.
[29] PDF No. 31-1416, International Centre for Diffraction Data, Newtown Square, USA.
[30] T.K. Campbell, E.R. Gilbert, G.D. White, G.F. Piepel, B.Y. Wrona, Nucl. Technol. 85 (1989) 160.
[31] G.D. White, C.A. Knox, E.R. Gilbert, A.B. Johnson Jr., Proceedings NRC Workshop on spent fuel/cladding reaction during dry storage, Gaithersburg, MD, [1983] (NUREG/CP-0049), p. 102.
[32] B.Ho. Kim, S.T. Hwang, K.Y. Lee, J. Korean Ind. Eng. Chem. 12 (2001) 300.
[33] PDF No. 45-433, International Centre for Diffraction Data, Newtown Square, USA.
[34] PDF No. 45-432, International Centre for Diffraction Data, Newtown Square, USA.
[35] V.K. Wadhavan, LATPAR, A Least Squares Program, Neutron Physics Division, Bhabha Atomic Research Centre, Mumbai, India, 1972.
[36] C.K. Gupta, H. Singh, Uranium Resource Processing: Secondary Resources, Springer, Berlin, 2003, p. 468.
[37] S. Suryanarayana, N. Kumar, Y.R. Bamanker, V.N. Vaidya, D.D. Sood, J. Nucl. Mater. 230 (1996) 140.
[38] P.A. Haas, W.B. Stines, U.S. Patent 4,409,157 (1983).